



CALORIMETRIC DETERMINATION OF PHOSPHOLIPID-MELITTIN INTERACTIONS

Linus N. Okoro

Keywords: Pressure perturbation calorimetry, DSC, coefficient of thermal expansion, volume change, phospholipids, Melittin.

The effect of melittin incorporated into the phospholipid bilayer of 1,2-dipalmitoyl-*sn*-glycero-3-phosphocholine (DPPC) at mole fractions up to 3.75 mol% have been investigated. The study reveals a considerable influence of melittin on the phase transition profile and volumetric properties of the DPPC bilayer. The temperature dependence of the coefficient of expansion, α , and the volume fluctuations of DPPC – melittin bilayer membranes in their different transition phases were determined by using pressure perturbation calorimetry (PPC), a relatively new and efficient technique, and differential scanning calorimetry (DSC). The experiments were carried out in the temperature range from 10 to 85 °C. Incorporating melittin up to 1.25 mol% into the lipid bilayer abolishes the pretransition. Remarkably, there is no shift in the transition temperature up to 2.5 mol% melittin, while more than one shoulder is observed at the low-temperature side of the DSC peak for 3.75 mol%, and a slight shift in melting temperature, T_m to 32°C. This could be linked to the lytic property of melittin at these high peptide concentrations.

* Corresponding Authors

E-Mail: linus.okoro@aun.edu.ng

[a] American University of Nigeria, Lamido Zubairu Way, Yola, Adamawa State, Nigeria

Introduction

Melittin

Melittin constitutes 50% of the dry weight of the honeybee venom. The active peptide melittin is released from its precursor, promelittin, during its biosynthesis in honey bee and later gets formylated.¹ It is a peptide composed of 26 amino acids (NH₂-G-I-G-A-V-L-K-V-L-T-T-G-L-P-A-L-I-S-W-I-K-R-K-R-Q-CONH₂) with no disulphide bridge, the N-terminal region (residues 1–20) is predominantly hydrophobic and the C-terminal region (residues 21–26) is hydrophilic due to the presence of a stretch of positively charged amino acids. Melittin is water soluble due to its amphiphilic property and yet it spontaneously associates with both natural and artificial membranes.² The crystal structures of melittin have been resolved by X-ray crystallography.³ It has been observed that in an aqueous solution of high peptide concentration, high pH value, or high ionic strength, tetrameric melittin of high symmetry is formed readily.²

Lipid – Melittin Interaction

Melittin causes bilayer micellization and membrane fusion and has also been observed to form voltage-dependent ion channels across planar lipid bilayers.^{4,5} The characteristic action of melittin is its hemolytic activity.^{6,7} It is commonly believed and accepted that multimeric pore formation is the mode of action of many naturally produced peptides such as antimicrobial peptides and toxins.^{8,9} The structure and function of such pores and their results show that melittin forms pores that have a rather wide distribution of sizes. For example, the sizes of the melittin pores that are characterized by the inner pore diameter have been reported to be in the range of 10–60 Å, 13–24 Å and 25–30 Å from vesicle leakage experiments.⁸ The diameter of these

pores is expected to increase when the peptide concentration is increased.

Under certain conditions, melittin molecules insert into the lipid bilayer and form multiple aggregated forms that are controlled by temperature, pH, ionic strength, lipid composition and the lipid-to-peptide ratio. It has been observed that lipid composition and phase separation appears to play a critical role in melittin-induced pore formation. The action of melittin on membrane proteins has been studied and apart from its ability to disrupt lipid bilayers, melittin affects the dynamics of membrane proteins. For instance, it has been reported that lytic concentrations of melittin dramatically reduce the rotational mobility of band 3 protein in human erythrocyte membranes.^{10,11}

Further DSC study has revealed membrane fusion between liposomes composed of acidic phospholipids and neutral phospholipids induced by melittin, in which the roles of hydrophobic and electrostatic interactions were investigated in membrane fusion induced by melittin.¹²

In this study, we investigated the influence of melittin incorporation on the thermodynamic and equilibrium volumetric properties of the 1,2-Dipalmitoyl-*sn*-glycero-3-phosphocholine (DPPC) bilayer membrane. To accomplish this, pressure perturbation calorimetry (PPC) has been used to determine the temperature dependence of the coefficient of expansion coefficient, α , as well as volume changes accompanying lipid phase transitions. DSC thermogram was also recorded to show the temperature-dependent phase changes.

Materials and methods

Sample Preparation

Multilamellar vesicles preparation for calorimetric studies

1,2-Dipalmitoyl-*sn*-glycero-3-phosphocholine (DPPC) was obtained from Avanti Polar Lipids (Alabaster, AL). Melittin

($\geq 97\%$ purity) as a lyophilized solid was obtained from Calbiochem (Germany). Both samples were used without further purification. Multilamellar vesicles (MLV) of DPPC and melittin with designated mole ratios were mixed in a chloroform-methanol mixture (3:1 v/v) and dried as a thin film under a stream of nitrogen and then freeze-dried in a freeze-dryer (Christ, Osterode, Germany) under high vacuum overnight. The lipid films were hydrated in a Tris buffer (10 mM Tris-HCl, 100 mM NaCl, pH 7.4), followed by vortexing at $\sim 62^\circ\text{C}$ (above the main phase transition temperature, T_m , of DPPC ($\sim 41.5^\circ\text{C}$ [Cevc 1987]), and five freeze-thaw cycles, resulting in homogeneous multilamellar vesicles (MLVs). The final DPPC concentration used in the calorimetric measurements was 5 mg/ml.

Calorimetric measurements

Differential scanning calorimetry

Pressure perturbation calorimetry and differential calorimetry measurements were performed with a MicroCal (Northampton, USA) VP-DSC micro-calorimeter, equipped with a pressurizing system from the same manufacturer.

The reference cell was filled with the Tris buffer solution. Both buffer and sample solutions were degassed before being injected into the respective cells. Included in the standard VP-DSC instrument is a pressuring cap that allows application of 1.8 bars to the cells in order to avoid air bubbles at elevated temperatures. The instrument was operated in the high gain mode at a scanning rate of 40°C h^{-1} . Baseline subtraction (pure buffer) and normalization with respect to scan rate and concentration were performed by the instrument software, yielding the temperature-dependent apparent (excess) molar heat capacity of the vesicles, C_p , with respect to the buffer solution.

Pressure perturbation calorimetry (PPC)

Pressure perturbation calorimetry (PPC) measurements were carried out on the VP-DSC calorimeter equipped with MicroCal's (Northampton, MA, USA) PPC accessory. A description of the technique and its potential applications is placed elsewhere [37-43]. This method enables the measurement of heat effects induced by small periodic changes of gas pressure ($\Delta p = \pm 5$ bar) above the solution.¹³⁻¹⁶ The physical principle is the same as in a heat-induced thermal expansion, although the measurable is ΔQ - the heat released upon a pressure change of Δp at temperature T . Three control and calibration measurements were performed, namely water (sample cell) versus water (reference cell), buffer versus water and buffer versus buffer. The results of these control experiments were fit by second-order polynomials and were used for the evaluation of the coefficient of thermal expansion $\alpha(T)$ of the measured system (fig. 1). From the relative volume changes $\Delta V/V$, the absolute volume changes ΔV can be determined when the specific volume and the molar mass of the sample are known.¹⁷

Knowing the thermal expansion coefficient of the solvent, α_0 , mass, m , and partial specific volume of the solute, V_s , through a series of reference measurements, one can calculate the apparent thermal expansion coefficient of the dissolved particles.

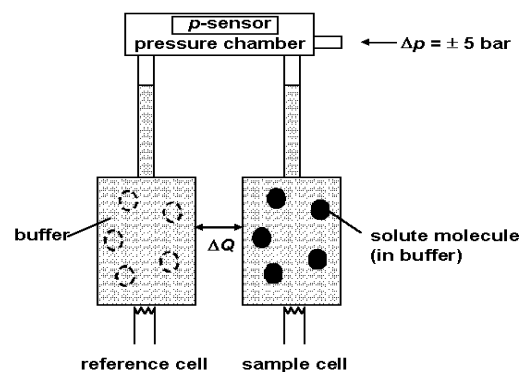


Figure 1. Schematic diagram of PPC describing the measurement curves and the derived thermodynamic parameters (*Microcal user note, 2000*).

Theory

The basic theory of pressure perturbation calorimetry is outlined below:

The heat of a reversible process, dQ_{rev} , is related to the entropy change, dS , at the temperature T .

$$dQ_{rev} = TdS \quad (1)$$

Differentiation with respect to pressure, p , yields

$$\left(\frac{\partial Q_{rev}}{\partial p}\right)_T = T\left(\frac{\partial S}{\partial p}\right)_T \quad (2)$$

From $dG = Vdp - SdT$, it follows that

$$\left(\frac{\partial S}{\partial p}\right)_T = -\left(\frac{\partial V}{\partial T}\right)_p \quad (3)$$

Eqn. (2) can thus be rewritten as

$$\left(\frac{\partial Q_{rev}}{\partial p}\right)_T = -T\left(\frac{\partial V}{\partial T}\right)_p \quad (4)$$

The thermal expansion coefficient of volume V is defined as

$$\alpha_v = \frac{1}{V}\left(\frac{\partial V}{\partial T}\right)_p \quad (5)$$

and can thus be determined from an isothermal measurement of the heat consumed or released upon a small pressure change:

$$\alpha_v = -\frac{\Delta Q_{rev}}{TV\Delta p} \quad (6)$$

Moreover, the relative volume change $\Delta V/V$ at a phase or structural transition, taking place in the temperature range from T_0 to T_e can be obtained by

$$\frac{\Delta V}{V} = \int_{T_0}^{T_e} \alpha(T) dT \quad (7)$$

For two-component systems, such as biopolymer solutions, one has to extend these equations [Lin 2002, Kujawa 2001]. If the sufficiently dilute solution is composed of m_s grams of a solute dissolved in m_0 grams of solvent, the total solution volume V may be expressed as

$$V = m_0 V_0 + m_s \bar{V}_s \quad (8)$$

where V_0 is the specific volume of the pure solvent, and V_s is the partial specific volume of the solute in the solution. The partial volume of the solute includes not just its intrinsic volume, but also any volume changes induced as a result of interactions with the solvent. Differentiating Eqn. (8) with respect to temperature at constant pressure yields

$$\left(\frac{\partial V_{total}}{\partial T} \right)_p = m_0 \left(\frac{\partial V_0}{\partial T} \right)_p + m_s \left(\frac{\partial \bar{V}_s}{\partial T} \right)_p \quad (9)$$

and after substituting the right hand side of Eq. (9) into Eq. (4) and (5), we obtain (10)

$$\left(\frac{\partial Q_{rev}}{\partial p} \right)_T = -T \left[m_0 \left(\frac{\partial V_0}{\partial T} \right)_p + m_s \left(\frac{\partial \bar{V}_s}{\partial T} \right)_p \right] = -T \left[m_0 V_0 \alpha_0 + m_s \bar{V}_s \bar{\alpha}_s \right] \quad (10)$$

where

$$\alpha_0 = (1/V) (\partial V_0 / \partial T)_p$$

is the α of the solvent volume and

$$\bar{\alpha}_s = (1/\bar{V}_s) (\partial \bar{V}_s / \partial T)_p$$

is the α of the solute partial volume. The heat arising from pressure perturbation of the solution can thus be viewed as the sum of that arising from the perturbation of the solvent and from the perturbation of the solute in solution. Integration of Eqn. (10) over a small pressure range Δp

$$\Delta Q_{rev} = -T \left[m_0 V_0 \alpha_0 + m_s \bar{V}_s \bar{\alpha}_s \right] \Delta p \quad (11)$$

leads to

In a differential PPC experiment, with sample solution in the sample cell and buffer in the reference cell, both cells are subjected to the same Δp so that the net heat change ΔQ_{rev} will be equal to the difference between Eqn. (11) for the sample cell and that for the reference cell. If the cells have an identical volume, then ΔQ_{rev} arises because the volume occupied by the solute in the sample cell, is replaced by solvent in the reference cell, *i.e.*,

$$\Delta Q_{rev} = -T (m_s \bar{V}_s \bar{\alpha}_s - m_s \bar{V}_s \alpha_0) \Delta p \quad (12)$$

which then rearranges to

$$\bar{\alpha}_s = \alpha_0 - \frac{\Delta Q_{rev}}{T m_s \bar{V}_s \Delta p} \quad (13)$$

where the total mass of solute, m_s , is obtained by multiplying its concentration, c_s [g/mL] with the cell volume, V_{cell} [mL].

Results and discussion

The excess heat capacity (C_p -profiles) of multilamellar vesicle (MLV) suspensions of DPPC with different concentrations of melittin added is displayed in figure 2. The heat capacity trace of pure DPPC displays a maximum at 41 °C, referred to as the main phase transition temperature, T_m . It is also observed that pure DPPC displays a small endothermic peak due to the L_{β} - P_{β} pretransition which appears around 35 °C. Overall, the heat capacity increase in the transition regime is mainly due to cooperative fluctuations of a large number of lipid molecules.

When the DPPC liposomes are prepared in the presence of melittin concentrations of 1 to 2.5 %, there is no change in the temperatures of the main transition.

Addition of 1 mol% melittin leads to a reduction of the lipid pre-transition peak. The peak is not completely abolished; however the temperature of the pre-transition shifts slightly to a lower temperature (32°C). The pre-transition is completely abolished at a melittin concentration of 1.25 mol% and at this particular concentration there appears a noticeable base peak broadening, a small asymmetry at the low-temperature wing and a reduction in transition profile which continues to increase with increasing melittin concentration. There is a concomitant reduction in the cooperativity of the chain melting transition, as a result of melittin incorporation, which is evidenced by the broadening of the transition profile. A shoulder (a small peak) appears at the low-temperature side (at 39 °C) of the main transition peak for 2.5 % melittin, with a further reduction of the transition profile and cooperativity.

Additionally, we observe no shift in the main transition temperature up to 2.5 mol% melittin. More than one shoulder is observed at the low-temperature side of the peak for 3.75 mol%, and a slight shift in T_m to 32°C. Oliynyk et al. observed a similar low-temperature shoulder in the C_p -

profile at higher melittin concentrations, in good agreement with our data.¹⁸

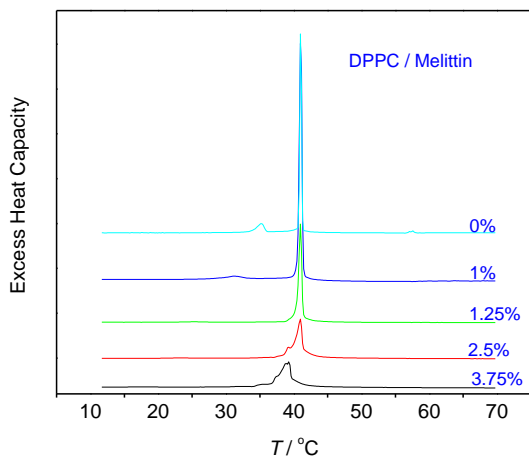


Figure 2. DSC thermograms of melittin in DPPC multilamellar vesicles

The PPC stacked plot of the coefficient of thermal expansivity versus temperature curves of the DPPC melittin mixtures is revealed in figure 3.

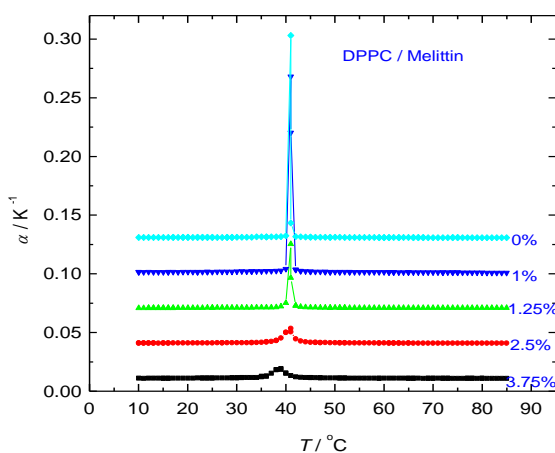


Figure 3. α , of DPPC/Melittin mixture

The PPC scans were carried out with solutions of DPPC/melittin in Tris buffer yielding the changes with temperature of the thermal expansion coefficient, α . The plots can be divided into three temperature regimes. We observe a slight increase in α below the pretransition with increase in melittin concentration, but not in any particular order.

For instance, as reported in our previous publication¹⁴, below the main phase transition temperature of pure DPPC, α increases slightly with increasing temperature. At the main phase transition temperature, α undergoes a rather sharp increase, reaches a maximum of about 0.15 K^{-1} at T_m (41°C), which then rapidly decreases with increasing temperature, to

reach a value close to that obtained below the transition temperature (α is $\sim 0.9 \cdot 10^{-3} \text{ K}^{-1}$ below the pretransition (20°C) and $\sim 1.0 \cdot 10^{-3} \text{ K}^{-1}$ above the main transition (65°C)). Similar α values for melittin concentrations 0% and 1% was observed. $\alpha = 1.01 \times 10^{-3} \text{ K}^{-1}$ for 2.5 mol%, and $\alpha = 1.12 \times 10^{-3} \text{ K}^{-1}$ for 3.75 mol% at 20°C . Above T_m (65°C), just below the pretransition, a very slight increase in α , with increase in melittin concentration (as an example, $\alpha = 0.92 \times 10^{-3} \text{ K}^{-1}$ and $\alpha = 1.02 \times 10^{-3} \text{ K}^{-1}$ at 65°C for 1.25 % and 2.5 % melittin respectively), whereas the main peak height of α in the transition region decreases and broadens markedly with increase in melittin concentration.

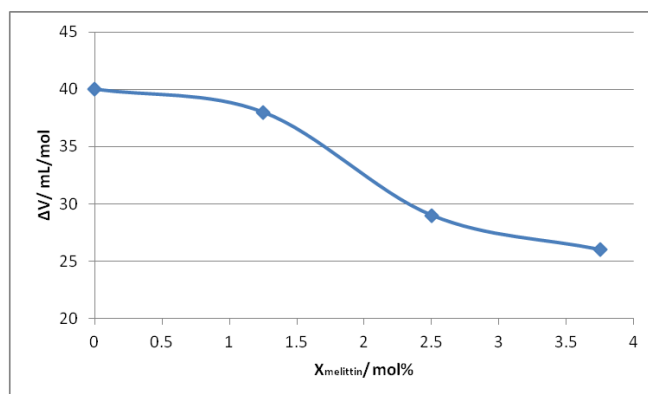


Figure 4. Concentration dependence of the absolute volume change, ΔV , of the DPPC/melittin mixtures

From the integration of α over the temperature range where the main transitions occur, we obtain the volume volume changes, ΔV , as shown in figure 4, for the pure DPPC and for each of the DPPC / melittin concentrations. $\Delta V/V = 0.04 \pm 0.007$ (4 %), which corresponds to an absolute volume change of 29 mL/mol, for pure DPPC, $\Delta V/V$ is 0.038 ± 0.001 for 1.25 mol%, 0.029 ± 0.002 for 2.5 mol%, and 0.026 ± 0.002 for 3.75 mol% melittin. The corresponding width of the overall transition, $\Delta T_{1/2}$, increases from about 1°C for the main transition of pure DPPC to about 3°C for the DPPC / 3.75 mol% melittin mixture.

Conclusion

The study has provided further insights into the disruptive effects of melittin on membrane bilayers having explored the use of calorimetry (pressure perturbation calorimetry and differential scanning calorimetry) to determine the absolute and relative volume change of DPPC – melittin bilayer membranes in their different phases.

We have shown that as the concentration of membrane-bound melittin increases, the relative volume change at the main transition of the lipid bilayer decreases. From the calorimetric measurements, upon incorporation of melittin into the lipid bilayer up to 1.25 %, it is observed that the pretransition is completely abolished. At this particular concentration, we observe a noticeable base peak broadening and a reduction in transition profile which continues with increase in melittin concentration. The appearance of a small endothermic peak at 39°C for 2.5 % melittin could possibly reflect morphological changes of free lipid vesicles in solution, the onset of the disruptive effect of melittin in DPPC bilayers. Remarkably, there is no

shift in the transition temperature up to 2.5 %, while more than one shoulder was observed at the low-temperature side of the peak for 3.75 %, and a slight shift in T_m to 32 °C. This implies a disordering effect, which could be attributed to melittin pore formation (disruptive effect), at this higher melittin concentration. At the main transition region, the peak height of α decreases and broadens markedly with increase in melittin concentration.

Peptides in both model and biological membranes have been observed to strongly affect the local state of the system, and the effect of peptide may equally depend on the overall state of the membrane.¹⁸ At the main transition region, the peak height of α decreases and broadens markedly with increase in melittin concentration.

Acknowledgement

Sincere grateful goes to Prof. Dr. R. Winter, Department of Physical Chemistry, Dortmund University of Technology, Germany, in whose laboratory this work was carried out. Financial support from the Deutsche Forschungsgemeinschaft (DFG), Germany and the regional county of Northrhine Westfalia is gratefully acknowledged.

REFERENCES

- ¹Habermann, E., *Science*, **1972**, *177*, 314-322.
- ²Dempsey, C. E., *Biochim. Biophys. Acta*. **1990**, *1031*, 143-161.
- ³Terwilliger, T.; Weissman L., and Eisenberg, D., *Biophys. J.* **1982**, *37*, 353-361.
- ⁴Bechinger, B. *J. Membr. Biol.* **1997**, *156*, 197-211.
- ⁵Monette, M. and Lafleur, M., *Biophys. J.*, **1995**, *68*, 187-195.
- ⁶Raghuraman H. and Chattopadhyay, A., *Chem. Phys. Lipids*, **2005**, *134*, 183-189.
- ⁷Rudenko S. V. and Patelaros, S. V., *Biochim. Biophys. Acta*, **1995**, *1235*, 1-9.
- ⁸Rex S., *Biophys. Chem.* **1996**, *58*, 75-85.
- ⁹Allende D., Simon, S. A. and McIntosh, T. J., *Biophys. J.*. **2005**, *88*, 1828-1837.
- ¹⁰Clague M. J. and Cherry, R. J., *Biochem. J.*, **1988**, *252*, 791-794.
- ¹¹Hui S. W., Stewart, C. M., and Cherry, R. J., *Biochim. Biophys. Acta*, **1990**, *1023*, 335-340.
- ¹²Bourinbaiar, A. S.; Coleman, C., *Arch Virol.*, **1997**, *142*, 2225-2235.
- ¹³Heerklotz, H. and seelig, J., *Biophys. J.*, **2002**, *82*, 1445-1452.
- ¹⁴Okoro, L. N. and Winter, R., *Z. Naturforsch.*, **2008**, *63b*, 769-778.
- ¹⁵Okoro, L. N., *Int. J. Chem.*, **2011**, *3(1)*, 166-175
- ¹⁶Okoro, L. N., *Can. J. Pure Appl. Sci.*, **2010**, *4(3)*, 1323 – 1332.
- ¹⁷Seemann, H. and Winter, R., *Z. Phys. Chem.* **2003**, *217*, 831-846.
- ¹⁸Oliylyk, V., kaatze, U. and Heimburg, T., *Biochim. Biophys. Acta* **2007**, *1768*, 236-245.

Received: 19.11.2012.

Accepted 17.12.2012.

